Advanced Steel Construction – Vol. 20 No. 3 (2024) 222–231
DOI:10.18057/IJASC.2024.20.3.2

UNIFIED FATIGUE LIFE CALCULATION OF Q460C STEEL FILLET WELD CRUCIFORM JOINTS CONSIDERING FATIGUE CRACK INITIATION AND PROPAGATION

Wan-Zhen Wang [1], Zhi-Yu Jie [1, *], Guo-Ji Yu [2], Lin-Feng Xiao [3] and Yu-Zhe Fan [1]

[1] *School of Civil Engineering, Geography and Environment, Ningbo University, Ningbo 315211, China*
[2] *Hongrun Construction Group Co., Ltd, Shanghai 200235, China*
[3] *Ningbo Huacong Architecture Design & Research Institute Co., Ltd, Ningbo 315042, China*
**(Corresponding author: E-mail: jiezhiyu@nbu.edu.cn)*

ABSTRACT

The present study experimentally investigates the effects of the relative stress amplitude and the relative nominal maximum stress on the fatigue life of Q460C steel fillet weld cruciform joints. An ellipsoidal fracture model proposed by the first author is used as the criterion of crack tip cracking and fatigue crack instability propagation. Theoretical calculations and numerical simulations were employed to analyze the fatigue crack initiation and propagation in the fillet weld cruciform joint. In addition, the fatigue crack initiation life, stable propagation life and total fatigue life were predicted using a unified fatigue life calculation model proposed by the first author. The calculation results reveal that the proposed unified fatigue life calculation model yield accurate fatigue life estimations, with errors ranging from −12.8% to −0.4%. Conversely, the calculation errors of the fatigue life formulas recommended in GB50017-2017, Eurocode3, and AISC360 range from −64.4% to −8.0%, −72.5% to −29.1%, and −49.4% to +30.7%, respectively.

ARTICLE HISTORY

Received: 13 November 2023
Revised: 7 February 2024
Accepted: 16 February 2024

KEYWORDS

Fillet weld;
Fatigue test;
Initiation life;
Stable propagation life;
Unified fatigue life calculation model

1. Introduction

Recently, high-strength steels have been increasingly used in civil engineering owing to their superior mechanical properties, including strength, ductility, toughness and fatigue. Welding stands out as the primary method of connecting steel structures, valued for its ease of fabrication and reliability in service. However, there are unavoidable defects and inherent residual stresses in the weld metal and heat-affected zone. Consequently, the welded joint may be vulnerable to fatigue damage under fluctuating loads. This has lead many researchers to study the fatigue properties of high-strength steels and their welded joints over the last several decades [1−16].

Many scholars have delved into the fatigue life calculation methodologies. Araujo et al. [1] proposed a new multiaxial fatigue model for fatigue strength estimation of high-strength steels with an average error not exceeding 16 %. Skriko et al. [2, 3] found through experiments that the current fatigue design codes and guidelines were applicable, albeit with somewhat conservatism, in assessing the fatigue strength of longitudinally loaded welded joints and fillet weld joints made of ultra-high-strength steel. The fatigue test results of high strength steel and its welded joint, investigated by Tong et al. [4, 5], indicated that high frequency loading tends to underestimate fatigue life, and fatigue strength of high strength steel surpasses that of ordinary steel. Wang et al. [6] presented a reliable high-cycle fatigue life assessment method for Q460D steel welded cruciform joints based on a unified crack growth approach. Lv et al. [7] found that the unified crack growth approach is able to provide a reliable fatigue life assessment for Q460C steel notched plates through fatigue tests and numerical simulations. Jie et al. [8] conducted experimental and numerical investigations on the fatigue properties of inclined cruciform joints with artificial pits, illustrating that the pitting corrosion damage reduces fatigue strength, but specimens without and those with smaller corrosion pits exhibited similar fatigue strengths at 2 million cycles. The pit depth and radius are the main parameters affecting the relative hot spot stress concentration factor. Guo et al. [9] proposed a fatigue reliability assessment method for the orthotropic steel deck based on a comprehensive vehicle load model and probabilistic multi-scale finite element analysis.

Additionally, the fatigue resistance of structural steel has been studied. Lipiäinen et al. [10] conducted fatigue test on component-sized hot-dip galvanized S960 cut edges and longitudinal welds, revealing that the surface quality has the most significant influence on the fatigue life after microscopic liquid metal embrittlement at the cut edges. Ahola et al. [11] experimentally investigated fatigue strength of non-load-carrying transverse attachment joints fabricated with single-sided fillet weld using of S355 and S1100 steel grades, and evaluated a fatigue life improvement technique for these joints comprising the use of a curved plate edge shape in the attachment. Yue et al. [12] carried out indoor acetic salt spray accelerated corrosion tests and high-cycle fatigue tests on Q690E high-strength steel and Q690qENH high-strength weathering steel. Their findings indicated that, under the same stress range, the fatigue life decreases with the increase of corrosion time. Sui et al. [13] studied the high-cycle S-N characteristics and fatigue cracking behaviors of 42CrMo steel with two different fine/coarse-grain tempered sorbite/bainite microstructures (FGM/CGM), and concluded that fatigue strength is greater for FGM than for CGM. Zhang et al. [14] performed microstructure characterization and fatigue crack propagation tests on the gradient surface-modified layer of high-strength steel. Their study demonstrated that increasing the depth of the surface-modified layer results in a decrease in yield strength and kernel average misorientation value, while the equivalent grain size of the slatted martensite structure and the number of the large-angle boundaries increase. Fang et al. [15] studied the crack-propagation mode and stress characteristics of stop-holes after drilling through fatigue tests and numerical simulations. The results indicated that stop-holes tend to crack in advance of the original crack reaching the edge of hole, with two cracks will propagating in opposite directions at a rapid rate until they meet. Drilling ahead of the crack increases the stress intensity factor at the crack tip by 15%, accelerating crack propagation and weakening the arresting effect. Yamada et al. [16] developed a technique, called impact crack closure retrofit (ICR) treatment, involving the closure of fatigue cracks by inducing plastic yielding at plate surface near fatigue cracks. Fatigue tests on various welded joints demonstrated how applying the ICR treatment improved fatigue life in the cracked welded joints.

The total fatigue life is typically determined by summing the initiation life and stable propagation life of fatigue cracks, excluding consideration the transient instability propagation life. Methods such as the Neuber model [17] and its modified versions, based on the local stress-strain, as well as the fracture mechanics principles such as the Paris-Erdogan law [18] and its modified forms, are commonly utilized. However, inconsistencies arise between the fatigue crack initiation life calculation based on the Neuber model and the fatigue crack propagation life calculation based on the Paris-Erdogan law due to differences in the definition of damage between these approaches.

Owing to the inadequate research on the limit states of fatigue crack initiation, propagation, and fracture in high-strength steels and their welded joints, current standards like China's code GB50017-2017 [19], AISC360 [20], and Eurocode3 [21] employ the allowable stress method and stress amplitude criterion to estimate fatigue life of high-strength steels and their welded joints.

These standards and previous studies fail to distinguish between fatigue crack initiation and propagation, despite variations in crack propagation rates before and after initiation in high-strength steels and their welded joints.

Fillet weld cruciform joints are largely used to connect beam webs and ribs in steel beam bridges. Utilizing high-strength steel in steel bridges allows for the design of smaller and thinner components, leading to steel savings and improved bridge aesthetics. The total fatigue life was divided into fatigue crack initiation life and fatigue crack stable propagation life. The ellipsoidal fracture model proposed by the first author [22] was employed as the criterion for determining crack tip cracking and fatigue crack instability propagation. Theoretical calculations and numerical simulations of fatigue cracking in the fillet weld cruciform joint were performed. Utilizing findings from literature [23, 24], the calculation model for fatigue crack initiation life and fatigue crack propagation life of Q460C steel fillet weld cruciform joints were derived, and the total fatigue life was obtained, leading to more accurate fatigue life calculations. The accuracy of the unified fatigue life calculation model was evaluated in comparison to the fatigue life formulas recommended in GB50017-2017, AISC360, and Eurocode3.

2. Fatigue tests of Q460C steel fillet weld cruciform joints

Fig. 1 shows the fillet weld cruciform joints using manual arc welding with Q460C steel and E5516-gas welding rods, according to GB50017-2017. The processed fillet weld cruciform joints are shown in Fig. 2.

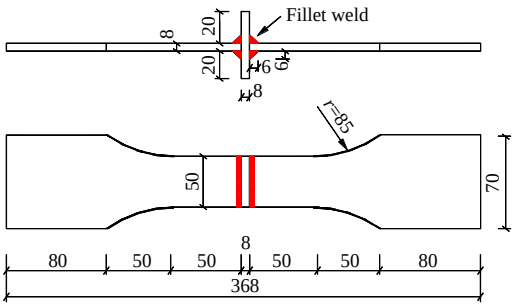

Fig. 1 Geometrical dimensions of the Q460C steel fillet weld cruciform joints

Fig. 2 Specimens of Q460C steel fillet weld cruciform joints

The measured length of the fillet weld (l_w), leg size (h_f), and loading parameters of each specimen are presented in Table 1. The effective bearing area of the fillet weld, denoted as A_{ew}, is equal to the fatigue fracture area (A_f), thus A_f=A_{ew}=0.7h_f×l_w. Additionally, f_{ys} and f_{uw} are the yield strength of the Q460C steel and the ultimate strength of the fillet weld, respectively. The maximum fatigue load (P_{max}) is calculated as A_p×σ_{max}=50×8×σ_{max}, while the minimum fatigue load (P_{min}) is expressed as 400×σ_{min}, where A_p is the cross-sectional area of the steel plate. It should be noted that the fatigue failure of the Q460C steel fillet weld cruciform joint is essentially a fracture problem under cyclic stress loading. In order to make the physical meaning of the parameters (σ_{max}, σ_{min}, $\Delta\sigma$) clearer, the loading parameters in this paper are defined as the ratio of the loading stress to the fracture strength of the fillet weld, namely σ_{max}/f_{fw}, σ_{min}/f_{fw}, and $\Delta\sigma/f_{fw}$, as opposed to the ratio of the loading stress to the yield strength of the fillet weld, σ_{max}/f_{yw}, σ_{min}/f_{yw}, and $\Delta\sigma/f_{yw}$. Tensile testing reveals that the fillet weld undergoes neck contraction upon reaching its ultimate strength f_{uw}, while the fracture strength f_{fw} is challenging to measure directly. Given that the mechanical properties of the fillet weld beyond its ultimate strength bear limited engineering significance, this paper conservatively approximates f_{fw}≈f_{uw}. Consequently, the loading stress parameters are expressed as σ_{max}/f_{uw}, σ_{min}/f_{uw} and $\Delta\sigma/f_{uw}$.

The mechanical properties of the Q460C steel and the fillet weld measured by the material properties test are listed in Table 2, including f_y (yield strength), f_u (ultimate strength), ε_y (yield strain), ε_u (ultimate strain), E (Young's modulus), and μ (Poisson's ratio).

Table 1
Geometrical and loading parameters of the Q460C steel fillet weld cruciform joints

Specimen No.	l_w (mm)	h_f (mm)	A_{ew} (mm²)	σ_{max}/f_{ys}	σ_{min}/f_{ys}	$\Delta\sigma/f_{ys}$	P_{max} (kN)	P_{min} (kN)	σ_{max}/f_{uw}	σ_{min}/f_{uw}	$\Delta\sigma/f_{uw}$
FWJ1	49.6	6.3	220.99	0.70	0.20	0.50	151.42	43.26	0.47	0.13	0.34
FWJ2	50.1	6.2	219.67	0.60	0.10	0.50	129.79	21.63	0.40	0.07	0.34
FWJ3	49.4	6.4	223.59	0.50	0.00	0.50	108.16	0.00	0.34	0.00	0.34
FWJ4	49.6	6.1	213.97	0.40	−0.10	0.50	86.53	−21.63	0.27	−0.07	0.34
FWJ5	49.7	6.3	221.44	0.30	−0.20	0.50	64.90	−43.26	0.20	−0.13	0.34
FWJ6	50.2	6.4	227.21	0.60	0.20	0.40	129.79	43.26	0.40	0.13	0.27
FWJ7	49.6	6.5	228.01	0.50	0.10	0.40	108.16	21.63	0.34	0.07	0.27
FWJ8	50.1	6.2	219.67	0.40	0.00	0.40	86.53	0.00	0.27	0.00	0.27
FWJ9	49.7	6.3	221.44	0.30	−0.10	0.40	64.90	−21.63	0.20	−0.07	0.27
FWJ10	49.8	6.1	214.84	0.20	−0.20	0.40	43.26	−43.26	0.13	−0.13	0.27
FWJ11	49.9	6.5	229.38	0.60	0.30	0.30	129.79	64.90	0.40	0.20	0.20
FWJ12	50.3	6.4	227.67	0.50	0.20	0.30	108.16	43.26	0.34	0.13	0.20
FWJ13	49.5	6.1	213.54	0.40	0.10	0.30	86.53	21.63	0.27	0.07	0.20
FWJ14	50.1	6.3	223.22	0.30	0.00	0.30	64.90	0.00	0.20	0.00	0.20
FWJ15	49.6	6.2	217.48	0.20	−0.10	0.30	43.26	−21.63	0.13	−0.07	0.20

Table 2
Materials properties of the Q460C steel and the fillet weld

Materials	f_y (MPa)	f_u (MPa)	ε_y (%)	ε_u (%)	E (GPa)	μ
Q460C steel	540.8	629.0	0.032	14.0	202.6	0.28
Fillet weld	719.2	802.2	0.041	15.8	206.8	0.27

The fatigue test of the Q460C steel fillet weld cruciform joint was carried out in compliance with China's code GB/T 3075-2008 [25]. The test setup, the fatigue crack initiation and propagation during the fatigue test, and fractured specimens are shown in Fig. 3. One end of specimen was fixed to the bottom fixture of a fatigue tester named SUNS890-500, while the other end was subjected to cyclic loading. Strain gauges (model: BX120-3AA) are pasted on both ends of the fillet weld, as shown in Fig. 3b, to collect the variation of strain along the loading direction of the weld root of the fillet weld with the number of cyclic loading. When the cracks initiated at the weld root of the fillet weld, the strain data would grow rapidly until the data overflowed. Therefore, loading was suspended before the strain data overflowed in this paper. A 150-fold scale microscope (precision: 0.01mm) was used to observe the fatigue crack initiation length (a_i≈0.05mm) at the weld root of the fillet weld, and the number of cyclic loadings at this time N_i was recorded. Subsequently, loading continued until the macro fatigue fracture of the Q460C steel fillet weld cruciform joint occurred.

The fatigue test results reveal that the fatigue crack initiates from the weld root at one end of the fillet weld, traverses the width of the effective bearing section of the fillet weld, and propagates along the length of the fillet weld to the other end within the effective bearing section. The effective bearing section of the fillet weld eventually experiences fatigue fracture.

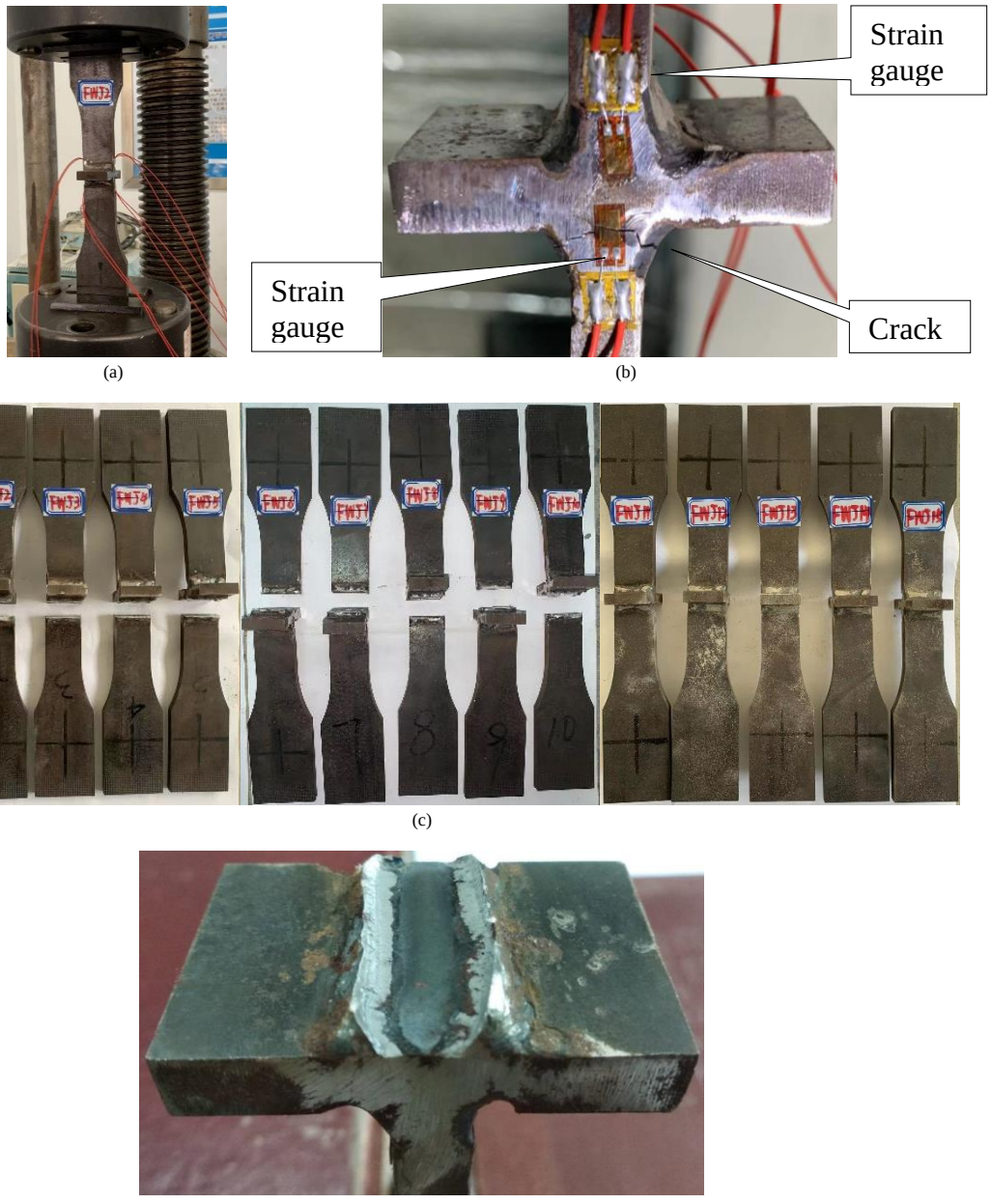

Fig. 3 Test setup and fatigue fracture of the Q460C steel fillet weld cruciform joints: a) Test setup; b) Crack initiation and propagation; c) Specimens A1−A16; d) Fatigue fracture

The fatigue crack initiation life ($N_{i,t}$), the total fatigue life ($N_{f,t}$), the fatigue crack stable propagation life ($N_{sp,t}$=$N_{f,t}$−$N_{i,t}$) obtained from fatigue testing, and the calculated fatigue life ($N_{f,\,GB}$, $N_{f,\,Eu}$, and $N_{f,\,AISC}$) based on Eqs. (1)~(3) recommended in GB50017-2017 (specimen type Z8: C_Z=0.72×10^{12}, β_Z=3), AISC360, and Eurocode3, respectively, for each specimen are presented in Table 3. The errors between the calculated fatigue life ($N_{f,\,GB}$, $N_{f,\,Eu}$, and $N_{f,\,AISC}$) and the tested total fatigue life ($N_{f,t}$), are denoted as $e_{GB\text{-}t}$, $e_{Eu\text{-}t}$, and $e_{AISC\text{-}t}$, respectively. The Eqs. (1)~(3) are presented below:

$$\lg N_{f,GB}=-3.0\lg\Delta\sigma+11.8573 \quad (1)$$

$$\lg N_{f,Eu}=-3.0\lg\Delta\sigma+12.0100 \quad (2)$$

$$\lg N_{f,AISC}=-3.0\lg\Delta\sigma+11.7444 \quad (3)$$

It is noted that the left side of Eqs. (1)~(3) is a dimensionless number, while the dimension of the right side is MPa, resulting in a dimensional discrepancy between both ends of Eqs. (1)~(3).

Table 3 reveals that the fatigue crack initiation life, the stable propagation life, and the total fatigue life of the Q460C steel fillet weld cruciform joint decrease with increasing σ_{max} and $\Delta\sigma$. As the nominal maximum stress and the stress amplitude rise, the stress at the weld root of the fillet weld increases, resulting in elevated fatigue crack initiation and propagation rates, leading to reduced fatigue crack initiation life, stable propagation life, and total fatigue life. Therefore, the influence of the stress amplitude and the nominal maximum stress should be considered in the fatigue life calculation of the Q460C steel fillet weld cruciform joint. The ratio of the fatigue crack initiation life to the total fatigue life ranges from 0.43 to 0.54.

The fatigue lives calculated by Eqs. (1) and (2) recommended in GB50017-2017 and AISC360 are too conservative for all specimens, with calculation errors ranging from −64.4% to −8.0% and −72.5% to −29.1%, respectively. Furthermore, the fatigue lives calculated by Eq. (3) recommended in Eurocode3 are conservative for some specimens ($\Delta\sigma/f_{uw}$<0.34 and σ_{max}/f_{uw}<0.34) and unsafe for others ($\Delta\sigma/f_{uw}\geq$ 0.34 or$\sigma_{max}/f_{uw}\geq$0.34). The overall calculation error exhibits a range of −49.4% to +30.7%.

Table 3
Fatigue test results of the Q460C steel fillet weld cruciform joints

Specimen No.	$N_{i,t}$ (cycles)	$N_{f,t}$ (cycles)	$N_{p,t}$ (cycles)	$N_{i,t}/N_{f,t}$	$N_{f,GB}$ (cycles)	e_{GB-t} (%)	$N_{f,AISC}$ (cycles)	e_{AISC-t} (%)	$N_{f,Eu}$ (cycles)	e_{Eu-t} (%)
FWJ1	17000	39600	22600	0.43	36415	−8.0	28079	−29.1	51758	+30.7
FWJ2	19500	42400	22900	0.46	36415	−14.1	28079	−33.8	51758	+22.1
FWJ3	23300	46600	23300	0.50	36415	−21.9	28079	−39.7	51758	+11.1
FWJ4	29300	53100	23800	0.55	36415	−31.4	28079	−47.1	51758	−2.5
FWJ5	36900	61400	24500	0.60	36415	−40.7	28079	−54.3	51758	−15.7
FWJ6	38500	98700	60200	0.39	71123	−27.9	54842	−44.4	101090	+2.4
FWJ7	43600	104600	61000	0.42	71123	−32.0	54842	−47.6	101090	−3.4
FWJ8	56400	118400	62000	0.48	71123	−39.9	54842	−53.7	101090	−14.6
FWJ9	73500	136700	63200	0.54	71123	−48.0	54842	−59.9	101090	−26.0
FWJ10	92200	156700	64500	0.59	71123	−54.6	54842	−65.0	101090	−35.5
FWJ11	106200	307800	201600	0.35	168588	−45.2	129995	−57.8	239622	−22.2
FWJ12	121100	325500	204400	0.37	168588	−48.2	129995	−60.1	239622	−26.4
FWJ13	152100	359600	207500	0.42	168588	−53.1	129995	−63.9	239622	−33.4
FWJ14	195200	406600	211400	0.48	168588	−58.5	129995	−68.0	239622	−41.1
FWJ15	257100	473300	216200	0.54	168588	−64.4	129995	−72.5	239622	−49.4

The fatigue properties of Q460C steel fillet weld cruciform joints surpass those of ordinary steel fillet weld cruciform joints. The fatigue crack initiation rate is lower than the fatigue crack propagation rate in the Q460C steel fillet weld cruciform joint. Achieving accurate fatigue life calculations for these joints entails separately calculating fatigue crack initiation life and stable propagation life. However, Eqs. (1)~(3) recommended in GB50017-2017, AISC360, Eurocode3 are formulated based on fatigue test data of ordinary structural steel fillet weld cruciform joints, lacking differentiate between fatigue crack initiation life and stable propagation life.

3. Unified fatigue life calculation model

The fatigue failure of the Q460C steel fillet weld cruciform joint is a process where repeated loading initiates an crack at the weld root of the fillet weld, which then extends and closes until the fatigue fracture due to insufficient net cross-section strength. Therefore, under normal circumstances, the fatigue failure of the Q460C steel fillet weld cruciform joint can be divided into three stages: fatigue crack initiation, stable propagation, and instability propagation.

In this study, the progression of the fatigue crack in the Q460C steel fillet weld cruciform joint, from initiation to stable propagation and then to instability propagation, is considered as a continuous, progressive, complete, and unified failure process in this paper. Therefore, it is reasonable to express the fatigue crack initiation life and stable propagation life as functions of the initiation size and stable propagation length of fatigue crack, respectively.

Wang [23] assumed that the fatigue crack initiation rate increases with the number of load cycles, and proposed a model to calculate the fatigue crack initiation life by integrating the fatigue crack initiation rate.

$$N_i=(a_i/\xi_i)^{1/\eta i} \quad (4)$$

Wang [24] proposed a fatigue crack stable propagation life calculation model based on the assumption that the fatigue crack stable propagation rate increases with the number of load cycles.

$$N_{sp}=(a_{sp}/\xi_{sp})^{1/\eta sp} \quad (5)$$

The unified fatigue life calculation model is derived from Eqs. (4) and (5).

$$N_f=N_i+N_{sp}=(a_i/\xi_i)^{1/\eta i}+(a_{sp}/\xi_{sp})^{1/\eta sp} \quad (6)$$

where N_i, N_{sp}, and N_f are dimensionless numbers that denotes the fatigue crack initiation life, stable propagation life and the total fatigue life, respectively. The parameters a_i and a_{sp} are the initiation size and stable propagation length of fatigue crack, respectively, measured in millimeters (mm). Additionally, ξ_i and ξ_{sp} are measurements related to the fatigue crack initiation mode and stable propagation mode, respectively, with dimensions in mm. η_i and η_{sp} are dimensionless numbers.

It is noted that both ends of Eqs. (4)~(6) are expressed as dimensionless numbers.

4. Unified fatigue life calculation of the Q460C steel fillet weld cruciform joints

The fatigue failure process of the Q460C steel fillet weld cruciform joints of is divided into three stages: fatigue crack initiation, stable propagation and instability propagation. Correspondingly, the fatigue fracture area, A_f, can be divided into fatigue crack initiation area, A_i (where $A_i=a_i\times h_e=0.05\times0.7h_f$, with a_i representing the fatigue crack initiation size and h_e denoting the width of the effective bearing section of the fillet weld), stable propagation area, A_{sp}, and instability propagation area, A_{ip}. Thus, A_f can be expressed as the sum of A_i, A_{sp}, and A_{ip}, given by the equation $A_f=A_i+A_{sp}+A_{ip}$.

The total fatigue life, N_f, can be divided into two distinct components: fatigue crack initiation life, N_i, and stable propagation life, N_{sp}. Given the brief duration of fatigue crack instability propagation life, it is not incorporated into this division. Therefore, the relationship is expressed as $N_f=N_i+N_{sp}$.

4.1. Calculation of fatigue crack stable propagation life

According to the fatigue crack stable propagation life calculation model suggested by Eq. (5), the parameters ξ_{sp} and η_{sp} are determined based on the fatigue crack stable propagation length, a_{sp}, and its corresponding fatigue crack stable propagation fatigue life, N_{sp}.

4.1.1. Calculation of fatigue crack stable propagation length

The fatigue crack instability propagation area can be obtained from the stress field within this area by employing the ellipsoidal fracture model proposed by the first author [22] as the criterion for fatigue crack instability propagation. Experimental findings reveal that the fatigue crack in the Q460C steel fillet weld cruciform joints traverses the width of the effective bearing section of the fillet weld. Consequently, the fatigue crack stable propagation area, $A_{sp}=A_f-A_0-A_i-A_{ip}$, can be used to calculate the fatigue crack stable propagation length, $a_{sp}=A_{sp}/h_e$, where A_0 is the area of initial defect. Upon examination of the tested specimens, no initial defects were identified, leading to the conclusion that $A_0=0$.

Wang [22] proposed an ellipsoidal fracture model coupled with an ellipsoidal yield model based on the assumption that fracture strength and yield strength of structural steel are equal when subjected to triaxial equal tensile stresses. This model is represented by Eqs. (7) and (8):

$$(\sigma_{seq}/r)^2+(\sigma_m/q)^2=3\tau_y^2 \tag{7}$$

$$\sigma_{seq}^2+(\sigma_m/q)^2=3\tau_y^2 \tag{8}$$

where $q=\frac{\sqrt{2}(1+\mu)}{3(1-2\mu)}$, $\tau_y=\frac{\sqrt{1+9q^2}}{3\sqrt{3}q}f_y$. r can be derived from $\frac{f_u}{f_y}\approx\frac{f_f}{f_y}=\frac{r\sqrt{1+9q^2}}{\sqrt{r^2+9q^2}}$. σ_{seq}, σ_m, τ_y, f_u, f_f, and f_y are the von Mises equivalent stress, mean stress, shear yield strength, uniaxial ultimate strength, uniaxial fracture strength, and uniaxial yield strength, respectively.

4.1.1.1. Theoretical calculation of fatigue crack stable propagation length

Fig. 4 shows the fatigue fracture model of fillet weld in the Q460C steel cruciform joint. The normal stress and shear stress at the effective bearing section of the fillet weld are given as follows:

$$\sigma_z=N/A_{up,tc}=1.414P_{max}/4A_{ip,tc} \tag{9}$$

$$\sigma_x=\mu_w\sigma_x=1.414\mu_wP_{max}/4A_{ip,tc} \tag{10}$$

$$\sigma_y=0 \tag{11}$$

$$\tau_{yz}=V/A_{up,tc}=1.414P_{max}/4A_{ip,tc} \tag{12}$$

$$\sigma_m=(\sigma_x+\sigma_y+\sigma_z)/3=1.414(1+\mu_w)P_{max}/12A_{ip,tc} \tag{13}$$

$$\sigma_{seq}=\sqrt{[(\sigma_x-\sigma_y)^2+(\sigma_y-\sigma_z)^2+(\sigma_z-\sigma_x)^2+6\tau_{yz}^2]/2}$$
$$=\sqrt{2\mu_w^2-2\mu_w+8}\times P_{max}/4A_{ip,tc} \tag{14}$$

where μ_w is the Poisson's ratio of the fillet weld.

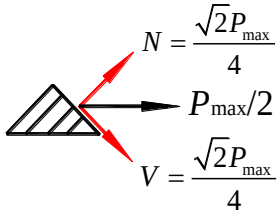

Fig. 4 Fatigue fracture model of fillet weld

The instability propagation area of the fatigue crack can be determined by substituting Eqs. (13) and (14) into Eq. (8), and the equation is rewritten as follows:

$$A_{up,tc}=\frac{\sqrt{9q_w^2(\mu_w^2-\mu_w+4)+(\mu_w+1)^2r_w^2}\times P_{max}}{6\sqrt{6}q_wr_w\tau_{yw}} \tag{15}$$

The parameters in Eq. (15) are calculated according to the tested material properties of the fillet weld listed in Table 2 as follows: $q_w\approx1.30$, $\tau_{yw}\approx428.65$MPa, and $r_w\approx1.12$.

The instability propagation area, the stable propagation area, and the stable propagation length of the fatigue crack are calculated theoretically as follows:

$$A_{sp,tc}=A_f-A_i-A_{ip,tc} \tag{16}$$

$$a_{sp,ct}=A_{sp,ct}/h_e \tag{17}$$

4.1.1.2. Numerical calculation of stable propagation length of fatigue crack

The finite element model of specimen FWJ2 employed to simulate the loading process of fatigue testing, constructed using a three-dimensional solid element Solid95 in ANSYS finite element software, is shown in Fig. 5. The first author [26] has verified the effectiveness of Solid95 for modeling fatigue crack propagation. A total of 60,289 elements and 193,567 nodes were modeled for mesh division. In alignment with the fatigue test methodology, the loading process entailed fixing one end while applying fatigue load to the other end.

The two horizontal steel plates and one vertical steel plate are bonded together by four fillet welds using the "GLUE" command in the ANSYS software to ensure a consistent deformation at the fused section between the fillet weld and the plate. At one edge of fillet weld in the finite element model, a column crack with a vertically penetrating semi-ellipsoidal cross section is implanted. The area of the semi-ellipsoid is denoted as $A_i+A_{sp,tc}$, with a semi-long axis defined as $a_c=a_i+a_{sp,tc}$, and a semi-short axis defined as $b_c=0.05a_c$, to simulate the theoretically calculated initiation and propagation length, $a_i+a_{sp,tc}$, and initiation and propagation area, $A_i+A_{sp,tc}$, of the fatigue crack in the fillet weld cruciform joint.

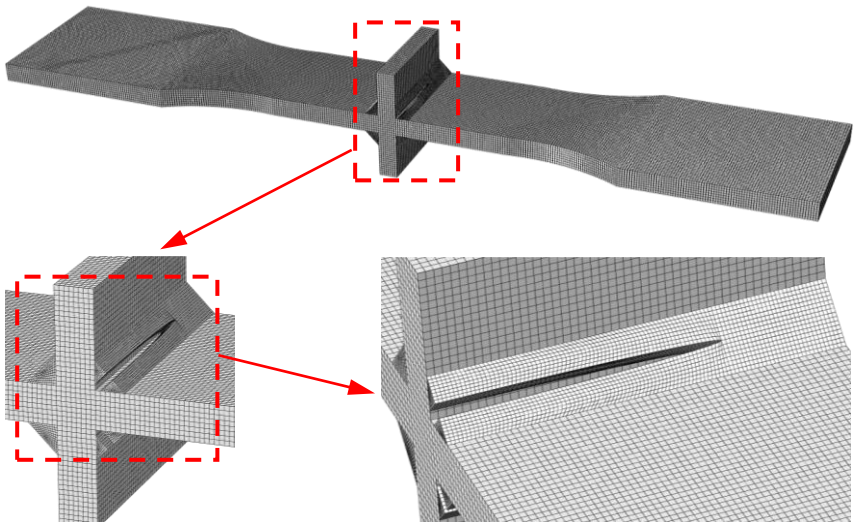

Fig. 5 Finite element meshes of specimen FWJ2

The ellipsoidal fracture model suggested by Eq. (7) was employed as the cracking criterion of the crack tip, while the "XFEM" module within the ANSYS finite element software was utilized to simulate the propagation and fatigue failure of the fatigue crack.

The fatigue cracking diagram of specimen FWJ2, obtained through numerical calculation, is presented in Fig. 6, accompanied by the corresponding stress field on the instability propagation area of fatigue crack. The fracture index, I_f, and the yield index, I_y, are calculated using Eqs. (7) and (8), respectively, as follows:

$$I_f = \sqrt{(\sigma_{seq}/r_w)^2 + (\sigma_m/q_w)^2}/\sqrt{3}\tau_{yw}\ ,\quad I_y = \sqrt{\sigma_{seq}^2 + (\sigma_m/q_w)^2}/\sqrt{3}\tau_{yw}\ .$$

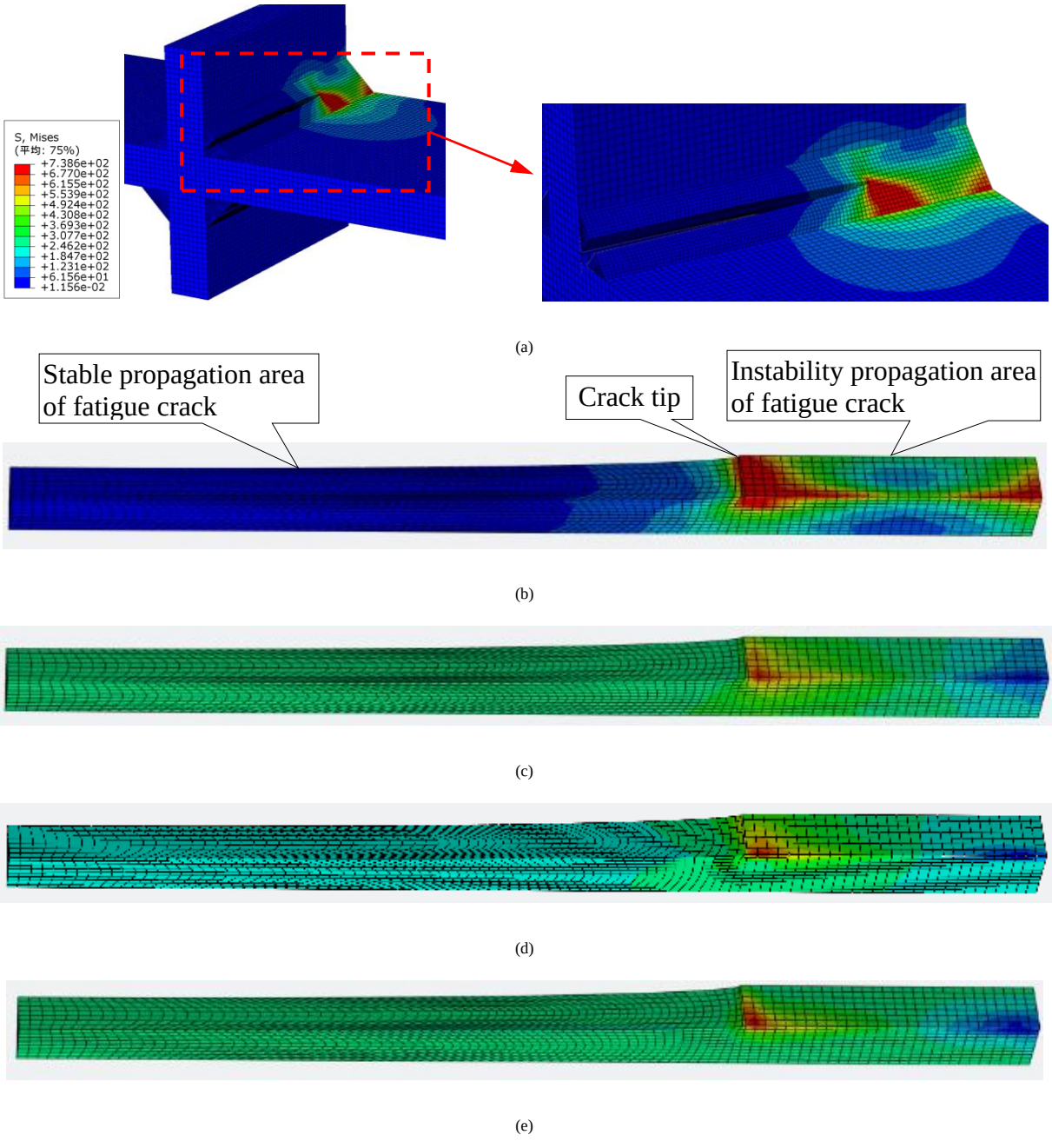

Fig. 6 Numerical calculated stress on the instability propagation area of fatigue crack in specimen FWJ2: a) Overall Mises equivalent stress; b) Mises equivalent stress; c) The first stress σ_1; d) The second stress σ_2; e) The third stress σ_3; f) The distribution of relative stress; g) The distribution of stress ratio, the fracture index, I_f, and the yield index, I_y.

Fig. 6a~e visually shows a high stress concentration at the crack tip. The peak values of the relative stresses, σ_1/f_{yw}, σ_2/f_{yw}, σ_{seq}/f_{yw}, and σ_m/f_{yw}, are all located at the crack tip, as shown in Fig. 6f. As can be seen from Fig. 6g, on the instability propagation area of fatigue crack, the stress triaxility ratio, σ_m/σ_{seq}, ranges from approximately 0.22 to 0.61, while stress constraint coefficient along the length of the butt weld, σ_2/σ_1, varies from about 0.11 to 0.67. Additionally, the stress constraint coefficient along the thickness of the butt weld is very small at this time. This suggests the presence of significant

constraint stresses on the instability propagation area of the fracture crack, particularly at the crack tip and along the length of the fillet weld. The instability propagation area of the fatigue crack has all entered the yield regime (I_y>1.0) and is on the verge of experiencing tensile transient fracture (I_f≥1.0).

4.1.2. Calculation of fatigue crack stable propagation life

The instability propagation area, A_{ip}, stable propagation area, A_{sp}, and stable propagation length, a_{sp}, of fatigue crack in the Q460C steel fillet weld cruciform joints, obtained from the numerical calculation, are listed in Table 4.

Table 4
Fitted parameters of fatigue crack propagation life calculation formula

Specimen No.	$N_{sp,t}$ (cycles)	A_f (mm^2)	A_{up} (mm^2)	A_{sp} (mm^2)	a_{sp} (mm)	η_{sp}	ξ_{sp} (10^{-10},mm)	s_{sp}	$\xi_{sp,0.95}$ (10^{-10},mm)	$N_{sp,c}$ (cycles)	$e_{sp,c-t}$ (%)
FWJ1	22600	220.99	74.81	146.18	32.8	3.18	5067.1	0.003	5217.5	20804	−7.9
FWJ2	22900	219.67	64.12	155.56	35.5	3.18	5067.1	0.003	5217.5	21320	−6.9
FWJ3	23300	223.59	53.43	170.16	37.6	3.18	5067.1	0.003	5217.5	21711	−6.8
FWJ4	23800	213.97	42.75	171.23	39.7	3.18	5067.1	0.003	5217.5	22084	−7.2
FWJ5	24500	221.44	32.06	189.38	42.5	3.18	5067.1	0.003	5217.5	22563	−7.9
FWJ6	60200	227.21	64.12	163.09	36.0	3.19	220.8	0.002	225.7	56608	−6.0
FWJ7	61000	228.01	53.43	174.57	38.0	3.19	220.8	0.002	225.7	57547	−5.7
FWJ8	62000	219.76	42.75	176.93	40.4	3.19	220.8	0.002	225.7	58652	−5.4
FWJ9	63200	221.44	32.06	189.38	42.5	3.19	220.8	0.002	225.7	59616	−5.7
FWJ10	64500	214.84	21.37	193.46	44.8	3.19	220.8	0.002	225.7	60626	−6.0
FWJ11	201600	229.38	64.12	165.27	36.0	3.20	4.1	0.002	4.2	197960	−1.8
FWJ12	204400	227.67	53.43	174.23	38.5	3.20	4.1	0.002	4.2	202247	−1.1
FWJ13	207500	213.54	42.75	170.80	39.6	3.20	4.1	0.002	4.2	204036	−1.7
FWJ14	211400	223.22	32.06	191.16	42.9	3.20	4.1	0.002	4.2	209241	−1.0
FWJ15	216200	217.48	21.37	196.11	44.7	3.20	4.1	0.002	4.2	211986	−1.9

The fatigue crack stable propagation life calculation model, as presented in Eq. (5), is derived by applying a double logarithm transformation to both sides of the equation.

$$\lg N_{sp,t}=(\lg a_{sp}-\lg\xi_{sp})/\eta_{sp} \tag{18}$$

The fatigue crack stable propagation life, $N_{sp,t}$, and stable propagation length, a_{sp}, are listed in Table 4. The fitted fatigue crack stable propagation life calculation formulas of specimens FWJ1−FWJ5, FWJ6−WJ10, and FWJ11−FWJ15 are derived accordingly (Fig. 7).

$$\lg N_{sp}=0.3151\lg a_{sp}+3.8736 \tag{19}$$

$$\lg N_{sp}=0.3148\lg a_{sp}+4.2885 \tag{20}$$

$$\lg N_{sp}=0.3133\lg a_{sp}+4.8157 \tag{21}$$

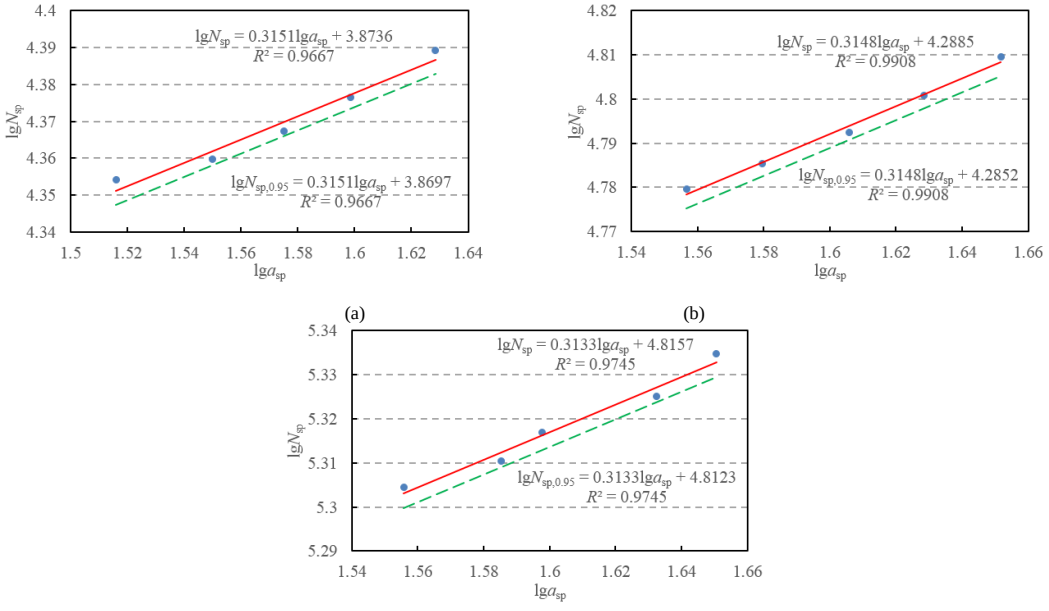

Fig. 7 Fitted fatigue crack stable propagation life calculation formula: a) Specimens FWJ1−FWJ5; b) Specimens FWJ6−FWJ10; and c) Specimens FWJ11−FWJ15

Table 4 presents the parameters ξ_{sp} and η_{sp} of the fatigue crack stable propagation life calculation formulas of specimens FWJ1–FWJ15, fitted from Eqs. (19) to (21).

The 1.645 times standard deviation, s_{sp}, corresponding to the fatigue crack stable propagation life of each parameter group was introduced into Eqs. (19) to (21). Subsequently, the fatigue crack stable propagation life, $N_{sp,t}$, and stable propagation critical length, a_{sp}, listed in Table 4, were refitted according to Eq. (18) to obtain the green dashed line equations in Fig. 7. The fitting fatigue crack stable propagation life calculation formulas for specimens FWJ1−FWJ5, FWJ6−WJ10, and FWJ11−FWJ15, with a confidence level of 95%, were obtained as follows:

$$\lg N_{sp}=0.3151\lg a_{sp}+3.8697 \tag{22}$$

$$\lg N_{sp}=0.3148\lg a_{sp}+4.2852 \quad (23)$$

$$\lg N_{sp}=0.3133\lg a_{sp}+4.8123 \quad (24)$$

The parameters $\xi_{sp,0.95}$ of the fatigue crack stable propagation life calculation formulas for specimens FWJ1−FWJ15, fitted from Eq. (22)−(24), are listed in Table 4. It can be seen that the parameter $\xi_{sp,0.95}$ increases as $\Delta\sigma/f_{uw}$ increases, and the parameter η_{sp} = 3.18−3.20. In this paper, the parameter η_{sp} is conservatively taken to be 3.19.

When $\Delta\sigma/f_{uw}$ = 0, it is a static loading condition, and the fatigue crack stable propagation life N_{sp} tends to infinity. According to Eq. (5), when $N_{sp}=\infty$, $\xi_{p,0.95}=0$.

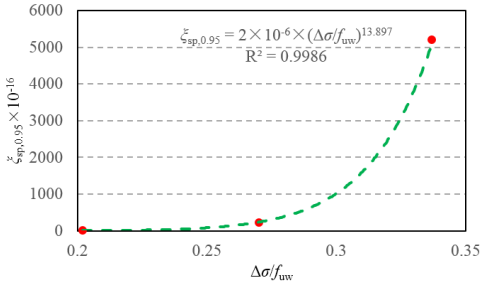

Fig. 8 Fitting function for the parameters $\xi_{p,0.95}$ and $\Delta\sigma/f_{uw}$

A fitting function for the parameters $\xi_{sp,0.95}$ and $\Delta\sigma/f_{uw}$ with the minimum variance, as shown in Fig. 8, is given by:

$$\xi_{sp,0.95}=2\times10^{-6}\times(\Delta\sigma/f_{uw})^{13.90} \quad (25)$$

Substituting Eq. (25) into Eq. (5) and considering η_{sp}=3.19, the fatigue crack stable propagation life calculation formula of the Q460C steel fillet weld cruciform joints can be expressed as follows:

$$N_{sp}=\left[\frac{a_{sp}}{2\times10^{-6}\times(\Delta\sigma/f_{uw})^{13.90}}\right]^{\frac{1}{3.19}} \quad (26)$$

The calculated fatigue crack stable propagation lives according to Eq. (26) are presented in Table 4, with a calculation error ranging from −7.9% to −1.0%. The overall calculation results are relatively safe and reliable.

4.2. Calculation of fatigue crack initiation life

The fatigue crack initiation life of the Q460C steel fillet weld cruciform joints, as listed in Table 3, increases as σ_{max}/f_{uw} and $\Delta\sigma/f_{uw}$ decrease. According to Eq. (4), the parameter η_i is related to the shape of the specimen and is thus independent of σ_{max}/f_{uw} and $\Delta\sigma/f_{uw}$. Therefore, the parameter ξ_i is related to σ_{max}/f_{uw} and $\Delta\sigma/f_{uw}$.

When σ_{max}/f_{uw}=1.0, the fillet weld directly fractures, resulting in the fatigue crack initiation life N_i=0. According to Eq. (4), when N_i=0, $\xi_i=\infty$. Conversely, when σ_{max}=0, implying no tensile stress in the fillet weld, the fatigue initiation life $N_i=\infty$. According to Eq. (4), when $N_i=\infty$, ξ_i=0.

Referring to the fatigue crack stable propagation length, a_{sp}, calculated by Eqs. (9) to (17), being a linear function of σ_{max}/f_{uw}, a function of the parameters ξ_i and σ_{max}/f_{uw}, satisfying the above conditions, is constructed as follows:

$$\xi_i=k_i\times\left(\frac{\sigma_{max}/f_{uw}}{1-\sigma_{max}/f_{uw}}\right)=k_i\times\left(\frac{\sigma_{max}}{f_{uw}-\sigma_{max}}\right) \quad (27)$$

where k_i is an undetermined coefficient.

Substituting Eq. (27) into Eq. (4) to then taking the logarithm of both sides simplifies the analysis:

$$\log N_i=\left[-\log\left(\frac{\sigma_{max}}{f_{uw}-\sigma_{max}}\right)+\log a_i-\log k_i\right]/\eta_i \quad (28)$$

The experimental data for the fatigue crack initiation life, $N_{i,t}$, and the ratio $\sigma_{max}/(f_{uw}-\sigma_{max})$ are fitted according to Eq. (28), depicted by the red solid line in Fig. 9.

$$\lg N_i=-0.6267\lg[\sigma_{max}/(f_{uw}-\sigma_{max})]+4.1914 \quad (29)$$

$$\lg N_i=-0.6203\lg[\sigma_{max}/(f_{uw}-\sigma_{max})]+4.4764 \quad (30)$$

$$\lg N_i=-0.6177\lg[\sigma_{max}/(f_{uw}-\sigma_{max})]+4.9141 \quad (31)$$

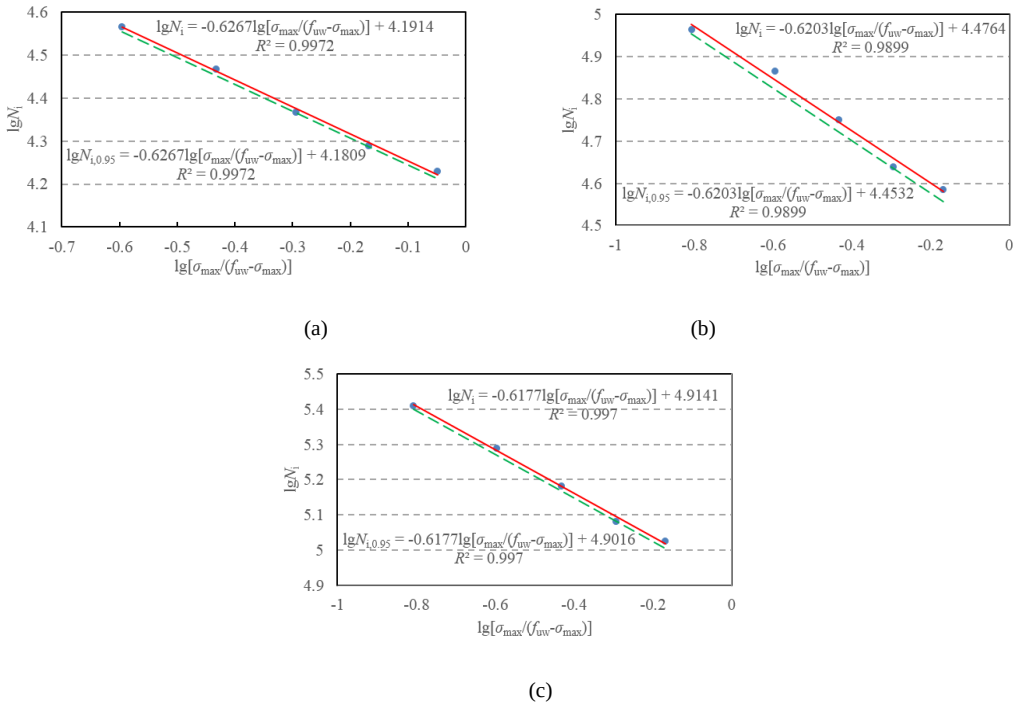

Fig. 9 Fitted fatigue crack initiation life calculation formula: a) Specimens FWJ1−FWJ5; b) Specimens FWJ6−FWJ10; c) Specimens FWJ11−FWJ15

According to Eqs. (29) to (31), with the fatigue crack initiation length a_i=0.05mm, the fitted parameters k_i and η_i are listed in Table 5.

Incorporating 1.645 times standard deviation, s_i, corresponding to the fatigue crack initiation life, into Eqs. (29) to (31), and the fatigue crack initiation life, $N_{i,t}$, and the ratio $\sigma_{max}/(f_{uw}-\sigma_{max})$, were refitted according to Eq. (27) to obtain the green dotted line equation in Fig. 9. Thus, the fatigue crack initiation life calculation formulas of specimens FWJ1−FWJ5, FWJ6−FWJ10F8, and FWJ11−WJ15, with a 95% confidence level, were obtained as follows:

$$\lg N_i=-0.6267\lg[\sigma_{max}/(f_{uw}-\sigma_{max})]+4.1809 \quad (32)$$

$$\lg N_i=-0.6203\lg[\sigma_{max}/(f_{uw}-\sigma_{max})]+4.4532 \quad (33)$$

$$\lg N_i=-0.6177\lg[\sigma_{max}/(f_{uw}-\sigma_{max})]+4.9016 \quad (34)$$

The parameters $k_{i,0.95}$, derived from Eqs. (32) to (34), are listed in Table 4. It can be seen that $k_{i,0.95}$ decreases as $\Delta\sigma/f_{uw}$ decreases. The parameter η_i exhibits minimal variation, ranging from 1.60 to 1.62. In this paper, η_i is conservatively taken to be 1.62.

Table 5
Fitted parameters of fatigue crack initiation life calculation formula

Specimen No.	$N_{i,t}$ (cycles)	η_i	k_i (10^{-8},mm)	s_i	$k_{i,0.95}$ (10^{-8},mm)	$N_{i,c}$ (cycles)	$e_{i,c\text{-}t}$ (%)	$N_{f,t}$ (cycles)	$N_{f,c}$ (cycles)	$e_{f,c\text{-}t}$ (%)
FWJ1	17000	1.60	102.5	0.006	106.6	14237	−16.3	39600	35041	−11.5
FWJ2	19500	1.60	102.5	0.006	106.6	16863	−13.5	42400	38183	−9.9
FWJ3	23300	1.60	102.5	0.006	106.6	20164	−13.5	46600	41875	−10.1
FWJ4	29300	1.60	102.5	0.006	106.6	24567	−16.2	53100	46651	−12.1
FWJ5	36900	1.60	102.5	0.006	106.6	30985	−16.0	61400	53547	−12.8
FWJ6	38500	1.61	30.4	0.014	33.1	37027	−3.8	98700	93635	−5.1
FWJ7	43600	1.61	30.4	0.014	33.1	44274	+1.5	104600	101821	−2.7
FWJ8	56400	1.61	30.4	0.014	33.1	53943	−4.4	118400	112595	−4.9
FWJ9	73500	1.61	30.4	0.014	33.1	68034	−7.4	136700	127649	−6.6
FWJ10	92200	1.61	30.4	0.014	33.1	91869	−0.4	156700	152495	−2.7
FWJ11	106200	1.62	5.5	0.008	5.8	102068	−3.9	307800	300028	−2.5
FWJ12	121100	1.62	5.5	0.008	5.8	122045	+0.8	325500	324292	−0.4
FWJ13	152100	1.62	5.5	0.008	5.8	148697	−2.2	359600	352733	−1.9
FWJ14	195200	1.62	5.5	0.008	5.8	187540	−3.9	406600	369782	−2.4
FWJ15	257100	1.62	5.5	0.008	5.8	253245	−1.5	473300	465231	−1.7

When $\Delta\sigma/f_{uw}=0$, representing a static loading condition, and the fatigue crack initiation life $N_i=+\infty$. According to Eqs. (4) and (27), when $N_i=+\infty$, $k_{i,0.95}=0$.

The relationship between $k_{i,0.95}$ and $\Delta\sigma/f_{uw}$ can be fitted using the data in Table 5, and the function should satisfy the boundary condition $k_{i,0.95}|_{\Delta\sigma/fuw=0}=0$. The fitted function is shown in Fig. 10.

$$k_{i,0.95}=5.45\times10^{-6}\times(\Delta\sigma/f_{uw})^{5.7} \quad (35)$$

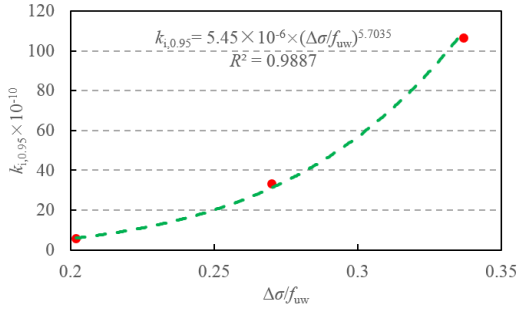

Fig. 10 Fitting function of the parameters $k_{i,0.95}$ and $\Delta\sigma/f_{uw}$

Substituting Eq. (35) into Eq. (27) and (4), and setting $\eta_i=1.62$, the fatigue crack initiation life calculation formula of the Q460C steel fillet weld cruciform joints is derived as follows:

$$N_i=\left[\frac{a_i}{5.45\times10^{-6}\times(\Delta\sigma/f_{wu})^{5.70}\times\left(\frac{\sigma_{max}}{f_{uw}-\sigma_{max}}\right)}\right]^{\frac{1}{1.62}} \quad (36)$$

The calculated fatigue crack initiation lives according to Eq. (36) are listed in Table 5, with a calculation error ranging from −16.3% to +1.5%.

4.3. Unified fatigue life calculation

Substituting Eqs. (26) and (36) into Eq. (6), the unified fatigue life calculation formula of the Q460C steel fillet weld cruciform joints is obtained as follows:

$$N_f=\left[\frac{a_i}{5.45\times10^{-6}\times(\Delta\sigma/f_{wu})^{5.70}\times\left(\frac{\sigma_{max}}{f_{uw}-\sigma_{max}}\right)}\right]^{\frac{1}{1.62}}+\left[\frac{a_{sp}}{2\times10^{-6}\times(\Delta\sigma/f_{uw})^{13.90}}\right]^{\frac{1}{3.19}} \quad (37)$$

The calculated total fatigue lives according to Eq. (37) and the corresponding calculation errors are listed in Table 5. The calculation error of Eq. (37) is from −12.8% to −0.4%, demonstrating that the calculation accuracy of Eq. (37) is better than that of Eqs. (1) to (3) recommended in GB50017-2017, AISC360, and Eurocode3.

5. Discussion

The ellipsoidal fracture model suggested by Eq. (8) serves as the criterion for crack tip cracking and instability propagation of fatigue crack. However, it is important to note that this model is specifically designed for isotropic structural steels characterized by equal tensile and compressive strengths. Therefore, the fatigue life assessment method presented in this paper, along with the fatigue initiation life calculation model, stable propagation life calculation model, and the total fatigue life model suggested by Eqs. (4) to (6), for the Q460C steel fillet weld cruciform joint, are only applicable to isotropic structural steels with uniform tensile and compressive strengths. They may not be applicable to engineered materials with different tensile and compressive strengths.

6. Conclusions

Fatigue tests were carried out on the Q460C steel fillet weld cruciform joints. The fatigue crack initiation length was obtained from the experimental analysis. The ellipsoidal fracture model was used as the crack tip cracking criteria and the instability propagation criterion of fatigue crack, and theoretical calculations and numerical simulations on the fatigue crack propagation in the fillet weld cruciform joint were employed. The fatigue life of the fillet weld cruciform joints was evaluated using the unified fatigue life calculation model and the fatigue life formulas recommended in GB50017-2017, Eurocode3, and AISC360. The following conclusions could be drawn:

1. A fatigue crack initiates at the root of the fillet weld due to the presence of a high stress concentration, and then fatigue fractures occur at the effective bearing section of the fillet weld.

2. The fatigue crack initiation life, $N_{i,t}$, stable propagation life, $N_{p,t}$, and total fatigue life, $N_{f,t}$, of the fillet weld cruciform joint decrease as the relative stress amplitude, $\Delta\sigma/f_{uw}$, and the relative nominal maximum stress, σ_{max}/f_{uw},

increase. The ratio of the fatigue crack initiation life to the total fatigue life ranges from 0.43 to 0.54.

3. The fatigue life formulas recommended in standards such as GB50017-2017, AISC360, and Eurocode3 are evaluated. The analysis revealed notable discrepancies between the calculated and tested fatigue lives, with calculation errors ranging from −64.4% to +30.7%. Specifically, the recommended formulas tend to be overly conservative, resulting in substantial underestimation of fatigue life.

4. The unified fatigue life calculation model provides more accurate predictions for the fatigue crack initiation life, stable propagation life, and total fatigue life of the fillet weld cruciform joint. The calculation errors associated with this model range from −16.3% to +1.5%, −7.9% to −1.0%, and −12.8% to −0.4%, respectively, indicating its superior performance compared to the recommended formulas.

Acknowledgement

The financial support provided by the Project of Science and Technology for Public Welfare of Ningbo City (Grant no. 2022S179, 2023S101), Zhejiang Provincial Natural Science Foundation of China (Grant no. LY24E080001), and China Postdoctoral Science Foundation (Grant no. 2023M742607) is gratefully acknowledged. The authors would like to express their sincere thanks for their support.

References

[1] Araujo LC, Malcher L, Oliveira D, et al. A new multiaxial fatigue endurance model for high strength steels taking into account the presence of small defects. Int J Fatigue 2024;178:107981.
[2] Skriko T, Lipiäinen K, Ahola A, et al. Fatigue strength of longitudinal load-carrying welds in beams made of ultra-high-strength steel. J Constr Steel Res 2021;179:106563.
[3] Skriko T, Ghafouri M, Bjoerk T. Fatigue strength of TIG-dressed ultra-high-strength steel fillet weld joints at high stress ratio. Int J Fatigue 2017; 94: 110–120.
[4] Tong LW, Niu LC, Ren ZZ, et al. Experimental investigation on fatigue behavior of butt-welded high-strength steel plates. Thin Wall Struct 2021;165:107956.
[5] Tong LW, Niu LC, Ren ZZ, et al. Experimental research on fatigue performance of high-strength structural steel series. J Constr Steel Res 2021; 183:106743.
[6] Wang WZ, Shi WZ, Li B, et al. High-cycle fatigue life assessment of welded cruciform joints of Q460D steel. Struct 2023;57(11):105163.
[7] Lv FJ, Wang WZ, Zhao W. Fatigue test and unified fatigue life calculation of Q460C steel notched plates. Build 2023;13(3):697.
[8] Jie ZY, Wang WJ, Zhuge P, et al. Fatigue performance of inclined cruciform welded joints with artificial pits. Adv Steel Constr 2021;17(1):20–27.
[9] Guo T, Liu ZX, Zhu JS. Fatigue reliability assessment of orthotropic steel bridge decks based on probabilistic multi-scale finite element analysis. Adv Steel Constr 2015;11(3):334–346.
[10] Lipiäinen K, Ahola A, Virolainen E, Hirvi A, et al. Fatigue strength of hot-dip galvanized S960 cut edges and longitudinal welds. J. Constr. Steel Res 2022;189:, 107083.
[11] Ahola A, Skriko T, Lipiäinen K, et al. On the weld root fatigue strength and improvement techniques for non-load-carrying transverse attachment joints with single-sided fillet welds and made of mild and ultra-high-strength steels. Eng Struct 2021; 249:113373.
[12] Yue YN, Shuling Gao SL, Li N, et al. High-cycle fatigue performance of corroded Q690E high strength steel and Q690qENH high-strength weathering steel. Constr and Build Mater 2023;401:132835.
[13] Sui GY, Wang ZQ, Li JR, et al. Roles of microstructures in high-cycle fatigue behaviors of 42CrMo high-strength steel under near-yield mean stress. Int J Fatigue 2023;177:107928.
[14] Zhang Y, Sang XG, Xu GT, et al. Fatigue crack propagation of the gradient surface-modified layer of high-strength steel. Int J Fatigue 2023;177:107921.
[15] Fang L, Fu ZQ, Ji, BH, et al. Propagation mode and characteristics of fatigue crack in steel bridge deck after drilling ahead of the crack tip. Adv Steel Constr 2022;18(2):544–551.
[16] Yamada K, Ishikawa T, Kakiichi T. Rehabilitation and improvement of fatigue life of welded joints by ICR treament. Adv Steel Constr 2015;11(3):2944–551.
[17] Neuber H. Theory of stress concentration for shear-strained prismatic bodies with arbitrary nonlinear stress-strain law. J App Mech 1961;28:544–550.
[18] Paris PC, Erdogan F. A critical analysis of crack growth laws. J Bas Eng 1963;85D:528–534.
[19] GB50017-2017, Standard for design of steel structures, Architecture Industrial Press of China, Beijing, China, 2017. (in Chinese)
[20] AISC-360-05, Specification for structural steel buildings, American Institute of Steel Construction, Chicago, 2005.
[21] Eurocode3-2005, EN 1993-1-9, Design of steel structures-fatigue strength of steel structures, British Standards Institution, London, 2005.
[22] Wang WZ. Crack criterion and fracture tests of structural steel. Eng Mech 2008;25:27–31. (in Chinese).
[23] Wang WZ. Calculation model of fatigue crack initiation life and fatigue life calculation of Q460C steel notched plates. Mater Rev 2024;38(4):23010056. (in Chinese).
[24] Wang WZ. Fatigue failure model of Q345 steel round bars. J Harb Inst Technol 2019;51: 58–64. (in Chinese).
[25] GB/T3075-2008, Metallic materials-fatigue testing-axial-force-controlled method, Standards Press of China, Beijing, 2008. (in Chinese)
[26] Wang WZ, Qian XD, Su RQ, et al. Tensile tests and analyses of notched specimens fabricated from high strength steels using a generalized yield model. Fatigue Fract Eng Mat Struct 2010;33:310–319.